The American Journal of Pathology, Vol. 174, No. 4, April 2009

DOI: 10.2353/ajpath.2009.080640

Immunopathology and Infectious Diseases

The Bacterial Virulence Factor Lymphostatin Compromises Intestinal Epithelial Barrier Function by Modulating Rho GTPases

Brian A. Babbin,* Maiko Sasaki,† Kirsten W. Gerner-Schmidt,* Asma Nusrat,* and Jan-Michael A. Klapproth†

From the Departments of Pathology and Laboratory Medicine and Medicine,† Division of Digestive Diseases, Emory University, Atlanta, Georgia*

Lymphocyte inhibitory factor A* (*lifA*) in *Citrobacter rodentium* encodes the large toxin lymphostatin, which contains two enzymatic motifs associated with bacterial pathogenesis, a glucosyltransferase and a protease. Our aim was to determine the effects of each lymphostatin motif on intestinal epithelial-barrier function. In-frame mutations of *C. rodentium lifA* glucosyltransferase (*Cr*GlM21) and protease (*Cr*PrM5) were generated by homologous recombination. Infection of both model intestinal epithelial monolayers and mice with *C. rodentium* wild type resulted in compromised epithelial barrier function and mislocalization of key intercellular junction proteins in the tight junction and adherens junction. In contrast, *Cr*GlM21 was impaired in its ability to reduce barrier function and influenced the tight junction proteins ZO-1 and occludin. *Cr*PrM5 demonstrated decreased effects on the adherens junction proteins β-catenin and E-cadherin. Analysis of the mechanisms revealed that *C. rodentium* wild type differentially influenced Rho GTPase activation, suppressed Cdc42 activation, and induced Rho GTPase activation. *Cr*GlM21 lost its suppressive effects on Cdc42 activation, whereas *Cr*PrM5 was unable to activate Rho signaling. Rescue experiments using constitutively active Cdc42 or C3 exotoxin to inhibit Rho GTPase supported a role of Rho GTPases in the epithelial barrier compromise induced by *C. rodentium*. Taken together, our results suggest that lymphostatin is a bacterial virulence factor that contributes to the disruption of intestinal epithelial-barrier function via the modulation of Rho GTPase activities. *(Am J Pathol 2009, 174:1347–1357; DOI: 10.2353/ajpath.2009.080640)

Enteric Gram-negative bacteria are a significant cause of intestinal inflammation and diarrhea worldwide. Pathogens such as enteropathogenic *Escherichia coli* (EPEC) or enterohemorrhagic *E. coli* (EHEC) are associated with significant morbidity and mortality in humans,[1] leading to dehydration and occasionally extraintestinal manifestations, including renal failure.[2] *Citrobacter rodentium*, a related mouse pathogen, functions as a model for human Gram-negative infection.[3] Like EPEC and EHEC, *C. rodentium* harbors a large pathogenicity island, termed locus for enterocyte effacement,[4] encoding for numerous effector proteins. After oral infection and adhesion to epithelial cells, Gram-negative enteric pathogens induce dense actin accumulation underneath the site of bacterial attachment and loss of microvilli, termed attaching and effacing lesions (A/E).[5] Furthermore, EPEC activates sophisticated mechanisms to breach the intestinal epithelial barrier.[6]

Previously, we have described a large immunomodulatory virulence factor in EPEC, termed lymphostatin, which suppresses cytokine expression *in vitro*.[7] Lymphostatin is encoded for by the *lifA* gene, which is present in *Chlamydia psittaci*, *Chlamydia muridarum*,[8] EPEC, EHEC,[9] and *C. rodentium*.[10] Lymphostatin expression has been associated with high virulence,[11] and has the strongest statistical association with diarrhea caused by atypical EPEC strains.[12] *lifA* consists of 9669 bp in EPEC and 9627 bp in *C. rodentium*, and encodes for three enzymatic motifs: a glucosyltransferase, a protease, and an aminotransferase motif. Infection with *C. rodentium* identified lymphostatin as an important bacterial effector protein regulating large bowel colonization and development of transmissible murine colonic hyperplasia.[10]

Supported by the Public Health Service (grants DK0628990-02, R24EK064399-04, and DK075392-01A2 to J.M.A.K.) and the National Institutes of Health (career development award K08 DK074706-01, grants DK55679 and 59888, and Digestive Diseases Research Development Center grant DK064399 to B.A.B.).

Accepted for publication December 11, 2008.

Address reprint requests to Jan-Michael A. Klapproth, M.D., Division of Digestive Diseases, Whitehead Biomedical Research Building, Suite 201, 615 Michael St., Atlanta, GA 30322. E-mail: jklappr@emory.edu.

Epithelial barrier function is maintained by two distinct structural protein complexes at apical intercellular junctions: tight junctions (TJ) and subjacent adherens junctions (AJ),[13] which are collectively referred to as the apical junctional complex (AJC). The AJC consists of transmembrane and cytoplasmic plaque proteins that associate with the actin cytoskeleton and play a pivotal role in regulating epithelial paracellular permeability.[14] The paracellular permeability is tightly controlled in diverse physiological and pathological states by signaling molecules that include diacylglycerol,[15] PKC,[16] protein kinase C,[17] Ca^{2+},[18] and small GTPases such as the Rho family of GTPases.[19] The Rho family of small GTPases encompasses three members, RhoA, Cdc42, and Rac1, which not only regulate AJC function but are also targeted by bacterial virulence factors.[20,21]

We demonstrate that *C. rodentium* is able to breach the intestinal epithelial barrier *in vivo* and disseminate systemically. Mutation of lymphostatin significantly impaired the ability of *C. rodentium* to colonize distant organs after intestinal infection. Our study suggests that lymphostatin contributes to disease pathogenesis and compromises the intestinal epithelial barrier *in vitro* and *in vivo* by modulating Rho GTPase activity and AJC structure.

Materials and Methods

In Vivo *Experiments*

All *in vivo* studies involving mice had prior approval by the Emory University Institutional Animal Care and Use Committee. Female, 4- to 6-week-old, pathogen-free C57BL/6 mice were purchased from The Jackson Laboratory (Bar Harbor, ME). Groups of five animals for each time point (days 2, 8, 14, and 20) were orally infected with a 100-μl suspension of $\sim 5 \times 10^8$ CFU *C. rodentium* wild type and EID3; control mice received phosphate-buffered saline (PBS) only.

lifA *Mutations*

Mutation of *lifA* in a region that does not encode for a known motif (EID3) has been previously described.[10] Because motifs encoded by *lifA* could not be expressed as a recombinant protein, we generated new glucosyltransferase and protease motif mutations, both of which have been implicated in bacterial pathogenesis.[21,22] Previously generated mutants GIM12 and PrM31 contained a stop codon (TAG) in position 2 of the scar sequence.[23] To replace the stop codon, 5′ primers Klapp-440 and -441 were designed to encode for leucine, used for polymerase chain reaction (PCR) amplification with downstream primers Klapp-167 and Klapp-170, respectively, and pKD4 as template.[10] PCR-amplified DNA (2 μg) was electroporated (2.5 kV) into *Cr*pKD46, recovered in SOC/10 mmol/L arabinose, and incubated at 42°C on LB agar with kanamicin. Insertion mutations were cured with 100 ng of pFT-A and heat-inactivated chlortetracycline (Sigma Chemicals Co., St. Louis, MO). Clones grown on plates without antibiotics were subjected to PCR and sequencing analysis. Scar sequences for clones *Cr*GIM21 and *Cr*PrM5 were determined to be in frame and encoded for TTG in codon 2 when sequenced in both directions.

Bacterial Proliferation, Epithelial Cell Adhesion, and Induction of A/E Lesions

C. rodentium wild type, *Cr*GIM21, and *Cr*PrM5 were diluted 1:100, OD_{600} measured, and serial dilutions plated on LB agar plates for up to 15 hours. CFU were enumerated the following day and the mean with SEM was calculated. For bacterial adhesion, confluent Caco-2 cells were infected with *C. rodentium* strains at MOI 1:10, washed after 3 hours, and lysed in 1% Triton X-100/PBS.[24,25] Serial dilutions were propagated on LB agar plates and enumerated the following day. Data are expressed as mean with SEM.

A/E lesions[10] were examined in 3T3 fibroblast cultures infected with EPEC E2348/69, *C. rodentium* wild type, and mutant strains at MOI 10:1. Cell cultures were fixed with 3.7% paraformaldehyde/PBS, permeabilized with 0.2% Saponin (Sigma), and blocked in 3% bovine serum albumin/0.2% Saponin/PBS. F-actin was labeled with phalloidin/Alexa 488 (1:1000; Invitrogen, Carlsbad, CA) and bacteria stained with 4′,6-diamidino-2-phenylindole. Stained 3T3 cultures were mounted in Prolong Gold (Invitrogen) and visualized with an Axioskope 2 plus scope (Zeiss, Jena, Germany).

Assessment of Epithelial Barrier Function

Transepithelial electrical resistance (TEER) was measured by EVOM (World Precision Instruments, Sarasota, FL) and paracellular permeability with fluoresceinated dextran (FD-3, MW 3000; Molecular Probes, Eugene, OR).[26] Monolayers were washed in Hanks' balanced salt solution ($HBSS^{+/+}$), 10 mmol/L HEPES, and equilibrated at 37°C, 10 minutes. After 5 hours of infection with MOI 10:1 *C. rodentium* strains, epithelial monolayers were loaded apically with 10 μg/ml of FD-3 and fluorescence intensity analyzed in aliquots from the lower chamber 60 minutes later (CytoFluor 2350 fluorescence measurement system; Millipore, Cambridge, MA). Control monolayer epithelial cell cultures were treated identically and instead of bacteria, 10 μl of PBS was added apically. TEER data are expressed as an average percentage change from baseline value with SEM. For fluorescein isothiocyanate (FITC)-dextran flux, numerical values from individual experiments were pooled and are expressed as mean with SEM.

Immunofluorescence Confocal Microscopy

Caco-2 cells were grown on polycarbonate membrane supports (Corning Inc., Corning, NY) to TEER $\sim$200 Ωs/cm^2. *C. rodentium* strains were added to the apical compartment of the Caco-2 monolayers, fixed/permeabilized in ice-cold 100% ethanol after 5 hours, and blocked with

3% bovine serum albumin/PBS at 4°C. F-actin was visualized with Alexa Fluor 488-conjugated phalloidin (Invitrogen), junctional proteins with primary antibodies at 1:1000 dilution (Invitrogen), and *C. rodentium* with *Citrobacter koseri* antibody (Cell Sciences, Canton, MA), 1:3000 dilution. Alexa Fluor 546- and 694-conjugated secondary goat antibodies, diluted 1:1000, were used for labeling of junctional proteins and bacteria. Samples were mounted in ProLong Gold (Invitrogen), images taken with Zeiss 510 confocal microscope and acquired with LSM image browser software (Carl Zeiss MicroImaging, Thornwood, NY). Images from three independent experiments were taken at identical detector gain settings for pixel intensity analysis, which was performed using the LSM 510 image analysis software (V 4.03).

Activation Status of Small GTPases

To determine Rac1, Cdc42, and Rho activity (Upstate, Charlottesville, VA), lysed monolayers were normalized for protein concentrations, and incubated with either recombinant PAK1-GST (Rac1, Cdc42) or Rhotekin-GST (RhoA, -B, -C) coupled to agarose beads (45 minutes, 4°C). This time point was chosen because it represented a 50% reduction in epithelial TEER from baseline. For Western blot analysis, rabbit polyclonal anti-Rac1, anti-Cdc42, or anti-Rho antibody beads (Santa Cruz Biotechnology, Santa Cruz, CA) were resuspended in sodium dodecyl sulfate sample buffer. Rho antibodies react with RhoA, -B, and -C and thus the term Rho is used to describe our results. Results of three independent Western blot analyses were subjected to densitometry and results expressed as mean with SEM.

Small GTPase Rescue Experiments

Activation of Cdc42-mediated signaling was achieved using a recombinant adenoviral vector encoding N-terminal myc-tagged constitutively active Cdc42.[27] Caco-2 cells were incubated in S-MEM/10% FBS (<10 μmol/L extracellular Ca^{++}) overnight and then placed into complete media with 5×10^5 plaque-forming U/ml viral particles for 2 days. Infection efficiency averaged ~70% (data not shown). Epithelial cell cultures were infected with *C. rodentium* wild type, MOI 1:10 and TEER determined by EVOM. Inhibition of Rho activity was performed using C3 exotoxin from *Clostridium botulinum*. Polarized Caco-2 cells were pre-incubated with 100 ng/ml of C3 exotoxin for 2 hours before infection with *C. rodentium* wild type in triplicate. TEER was measured throughout a 15-hour time course. Data are expressed as the mean with SEM of the percent change from baseline TEER from three independent experiments.

In Vivo *Immunofluorescence Microscopy*

For each condition and time point (days 8 and 14), three C57BL/6 female mice at 4 weeks of age were infected with 5×10^8 CFU of *C. rodentium* wild type, *Cr*GIM21, and *Cr*PrM5 in 100 μl of PBS via oral gavage. Control animals received 100 μl of PBS alone. On days 8 and 14 the distal half of the colon was resected and fecal matter removed. Colon specimens were embedded in OCT medium (Sakura Finetechnical Company, Tokyo, Japan) and cut into 6-μm frozen sections with a cryostat (Leica Microsystems, Nussloch, Germany). Samples were fixed with 100% ethanol for 5 minutes at −20°C. Slides were blocked in 3% bovine serum albumin, 0.1% saponin in PBS for 1 hour at room temperature. Junctional proteins were labeled with polyclonal antibodies directed against β-catenin (Sigma) and occludin (Invitrogen) at 1:250 dilution for 1 hour followed by secondary goat anti-rabbit Alexa 488 antibody (1:1000 dilution, Invitrogen) for 30 minutes at room temperature. Junctional proteins were visualized using an AxioCam MRc microscope (Zeiss) loaded with Axiovision MRc and microscopic images analyzed using Axiovision (Rel. 4.6).

Statistical Analysis

Nonparametric analysis was performed by Student's *t*-test for all data. Differences were considered significant if P was ≤ 0.05.

Results

Lymphostatin Contributes to the Ability of C. rodentium *to Compromise the Intestinal Epithelial Barrier* in Vivo *and Systemically Disseminate*

Although infection of mice with *C. rodentium* is generally thought to be confined to the mucosal surface of the colon, some studies have identified dissemination of this pathogen to extra-intestinal sites.[28] Similarly, our *in vivo* studies revealed colonization of extra-intestinal sites by *C. rodentium*. *C. rodentium* wild type was recovered from splenic tissues at 996 CFU/organ on day 2 after oral administration of the pathogen, which increased to 32,152 CFU/organ by day 8 after infection. By days 14 and 20 splenic colonization was decreased to 712 CFU/organ and 196 CFU/organ, respectively (Figure 1). Interestingly, infectious counts for a lymphostatin mutant, *lifA* EID3, were significantly lower at all time points investigated: day 2, 368 CFU/organ; days 8 and 14, 72 CFU/organ; day 20, 8 CFU/organ ($P < 0.05$). Results were similar for mesenteric lymph nodes and liver (data not shown). Thus, these findings suggest that lymphostatin plays a role in the ability of *C. rodentium* to cross the intestinal epithelial barrier and colonize extra-intestinal organs.

Given the implication of lymphostatin in mediating the *C. rodentium*-induced compromise in intestinal epithelial barrier function and systemic infection, we sought to determine whether *C. rodentium* infection results in disruption of the AJC and if lymphostatin contributes to such an effect. For these studies, we generated two new *C. rodentium* lymphostatin mutants with in frame mutations of *lifA* glucosyltransferase motif (*Cr*GIM21) and protease

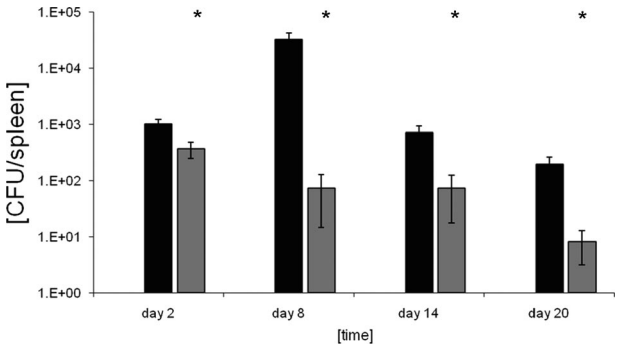

Figure 1. *C. rodentium* lymphostatin plays a role in extra-intestinal colonization. Splenic CFU for *C. rodentium* wild type (black bars) were 996 CFU/organ on day 2, which increased to 32,152 CFU/organ on day 8. By days 14 and 20 splenic colonization was decreased to 712 CFU/organ and 196 CFU/organ, respectively. Infectious counts for mutant EID3 (gray bars) were significantly lower at all time points investigated: day 2, 368 CFU/organ; days 8 and 14, 72 CFU/organ; day 20, 8 CFU/organ (*$P < 0.05$). Gram-negative growth was not detected at any time in spleen cultures from control mice gavaged with 100 μl of PBS (white bars).

motif (*Cr*PrM5), both of which have been implicated in bacterial pathogenesis (Figure 2).

C. rodentium *Lymphostatin Mutants Retain Basic Pathogenicity Features*

To determine whether mutations in *C. rodentium* lymphostatin influence basic bacterial functions, we first examined growth curves of mutant strains *Cr*GIM21 and *Cr*PrM5 in comparison with those of *C. rodentium* wild type for up to 15 hours. Proliferation of *C. rodentium* wild type, *Cr*GIM21, and *Cr*PrM5 strains were indistinguishable during lag (0 to 2 hours), log (2 to 9 hours), and plateau phase (9 to 13 hours) as determined by OD_{600} (Figure 3A) and by plating of serial dilutions on LB agar plates on analysis the following day.

Lymphostatin has also been characterized as an adhesion factor for EHEC serotype O111:H−.[25] Mutation of O111:H− lymphostatin lead to an almost sevenfold reduction in bacterial adhesion to CHO cells *in vitro*. We therefore examined whether mutation of *C. rodentium* lymphostatin impairs its ability to adhere to intestinal epithelial cells. No significant difference was observed in bacterial-epithelial adhesion after infection of the polarized model intestinal epithelial cell line, Caco-2, with *C. rodentium* wild type and mutant strains (data not shown). Mean CFU/1 $\times$ 10^6 Caco-2 epithelial cells from three independent experiments were 1.9 $\times$ 10^6 for *C. rodentium* wild type, 1.42 $\times$ 10^6 for *Cr*GIM21, and 1.47 $\times$ 10^6 for *Cr*PrM5 ($P > 0.05$).

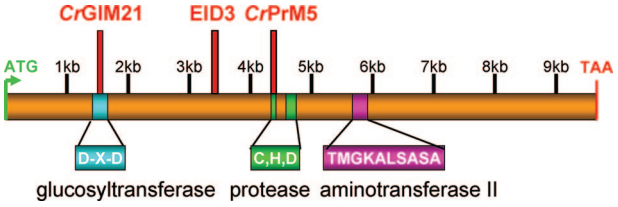

Figure 2. *lifA* in *C. rodentium*. *C. rodentium lifA* is 9627 bp in size, encoding for a putative 364-kDa protein with three distinct motifs: glucosyltransferase (1.6 kb, DXD), protease motif (4.5 to 4.8 kb, C, H, D), and aminotransferase II (5.8 kb, TMGKALSASA). We generated three mutations in *C. rodentium lifA*: *Cr*GlM21 at 1.6 kb, EID3 at 3.5 kb, and *Cr*PrM5 at 4.5 kb.

Next, we determined whether mutation of lymphostatin glucosyltransferase or protease motifs impairs the ability of *C. rodentium* to form attaching and effacing (A/E) lesions. For these experiments, we used 3T3 fibroblasts, which have been classically used for such studies, and bacterial strain E2348/69 was used as a positive control. *C. rodentium* wild type and both lymphostatin mutants were able to form A/E lesions similar to E2348/69 (Figure 3B). Taken together, the above results support that the basic yet critical pathogenic properties of *C. rodentium* are not altered by inactivating either the lymphostatin glucosyltransferase or protease motifs.

Effects of C. rodentium *and Lymphostatin Mutants on Epithelial Barrier Function*

Because *C. rodentium* demonstrated the ability to compromise the intestinal epithelial barrier and disseminate in mice, we analyzed the effects of *C. rodentium* wild type, *Cr*GIM21, and *Cr*PrM5 on intestinal epithelial barrier properties. TEER of monolayers was measured for up to 15 hours after infection. Infection with all three *C. rodentium* strains, ultimately resulted in a significant and sustained decrease in TEER (Figure 4A). However, the decrease in TEER observed after infection with *Cr*GIM21 was on average 20% reduced after 6 hours compared with infections with *C. rodentium* wild type and *Cr*PrM5.

Subsequently, we assessed paracellular permeability of FITC-dextran across the epithelial monolayers after infection with *C. rodentium* wild type or the lymphostatin mutant strains. Paracellular flux of FITC-dextran increased in response to *C. rodentium* wild type and both mutants. However, the degree of dextran flux was attenuated after *Cr*GIM21 infection compared with *C. rodentium* wild type and *Cr*PrM5, consistent with the TEER results (Figure 4B, $P < 0.05$). Because mutation of the lymphostatin glucosyltransferase motif attenuated the decrease in TEER and increased FITC-dextran flux in response to *C. rodentium* infection, these data implicate a role of *C. rodentium* lymphostatin in compromising the intestinal epithelial barrier.

Lymphostatin Plays a Role in the Disruption of the AJC in Vitro

Given that infection with *C. rodentium* wild type and lymphostatin mutants compromised epithelial barrier function, we next analyzed their influence on the localization and expression of key AJC proteins including ZO-1, occludin, E-cadherin, and β-catenin. Infection with *C. rodentium* wild type resulted in a significant redistribution of these apically located TJ and AJ proteins away from intercellular contacts in areas of high bacterial colonization (Figure 5, A and B). Both lymphostatin mutants disrupted the localization of TJ and AJ proteins. However, redistribution of apical ZO-1 and occludin away from TJs was dramatically attenuated with *Cr*GIM21 infection com-

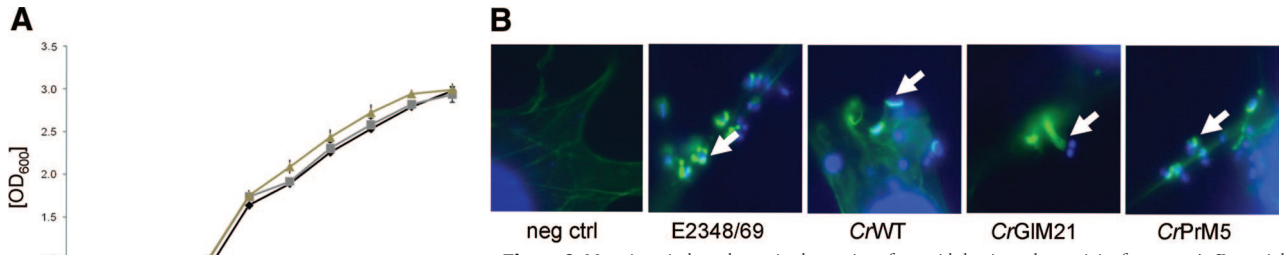

Figure 3. Mutations in lymphostatin do not interfere with basic pathogenicity features. **A:** Bacterial proliferation of *C. rodentium* wild type (open diamonds), *Cr*GIM21 (closed squares), and *Cr*PrM5 (closed triangles) strains was indistinguishable during lag (0 to 2 hours), log (2 to 9 hours), and plateau phase (9 to 13 hours) as determined by OD_{600} and plating of serial dilutions on LB agar (data not shown). **B:** Mutations of lymphostatin glucosyltransferase (*Cr*GIM21) and protease motif (*Cr*PrM5) did not interfere with formation of A/E lesions in 3T3 fibroblast cultures (**white arrows**) in comparison with *C. rodentium* wild type (*Cr*WT) and EPEC strain E2348/69.

pared with *C. rodentium* wild type and *Cr*PrM5 (Figure 5A), even in areas of high bacterial density (Figure 5A, white arrows). Pixel intensity analysis revealed a 5.3- and 5.4-fold decrease in the TJ localization of ZO-1 after infection with *C. rodentium* wild type and *Cr*PrM5, respectively, whereas *Cr*GIM21 infection had an insignificant effect on ZO-1 localization (Figure 5B, $P < 0.05$). Similar results were obtained for occludin in that *C. rodentium* wild type and *Cr*PrM5 induced a 3.6- and 3.5-fold decrease in occludin staining intensity at TJs, respectively, whereas infection with *Cr*GIM21 resulted in a decrease in the redistribution of occludin from TJs compared with wild type and *Cr*PrM5 (Figure 5B, $P < 0.05$). Disruption of apical and perijunctional F-actin architecture mirrored findings for ZO-1 and occludin. Microscopic analysis of the basolateral F-actin distribution showed an intact intestinal epithelial monolayer without individual cell drop out (Figure 5A, middle). Western blot analysis revealed that the average protein concentrations of the TJ protein ZO-1 decreased by 46%, 31%, and 13% in *C. rodentium* wild type-, *Cr*GIM21-, and *Cr*PrM5-infected cell cultures, respectively, compared with negative controls (Figure 5C, $P < 0.05$). Occludin protein expression showed a similar decline, ranging from 21 to 45% in infected monolayer cultures ($P < 0.05$). Expression of β-actin was not affected and remained stable in control cultures and during incubation with *C. rodentium* wild type, *Cr*GIM21, and *Cr*PrM5.

In contrast to the findings for the TJ proteins, significant redistribution of β-catenin and E-cadherin away from AJs was observed after infection with *C. rodentium* wild type and *Cr*GIM21 but not during infection with *Cr*PrM5 (Figure 6A). Disruption of subcortical F-actin mirrored findings for β-catenin and E-cadherin during infection with wild-type and lymphostatin mutant strains with an intact monolayer structure (Figure 6A, middle). These changes occurred in areas where large numbers of bacterial colonies were attached to the surface of epithelial cells (Figure 6A, white arrows). Pixel intensity analysis from three independent experiments showed a 2.3-fold and 2.5-fold reduction for apically located β-catenin and E-cadherin immunostaining, respectively, in response to infection with *C. rodentium* wild type and *Cr*GIM21, but not for *Cr*PrM5 (Figure 6B, $P < 0.05$). This was also the case for E-cadherin redistribution because incubation with *C. rodentium* wild type and *Cr*GIM21 leads to a threefold and twofold reduction of this AJ protein member, which was statistically significant in comparison with infection with CrPrM5 (Figure 6B, $P < 0.05$). In comparison with negative control cultures, Western blot analysis revealed that total levels of β-catenin protein decreased by 30% for cultures infected with *C. rodentium* wild type and mutant *lifA* strains (Figure 6C, $P < 0.05$). E-cadherin and β-actin protein expression remained stable throughout the experiments (Figure 6C). Thus, the above findings suggest that lymphostatin plays a role in the disruption of the AJC structure. Although both lymphostatin mutants

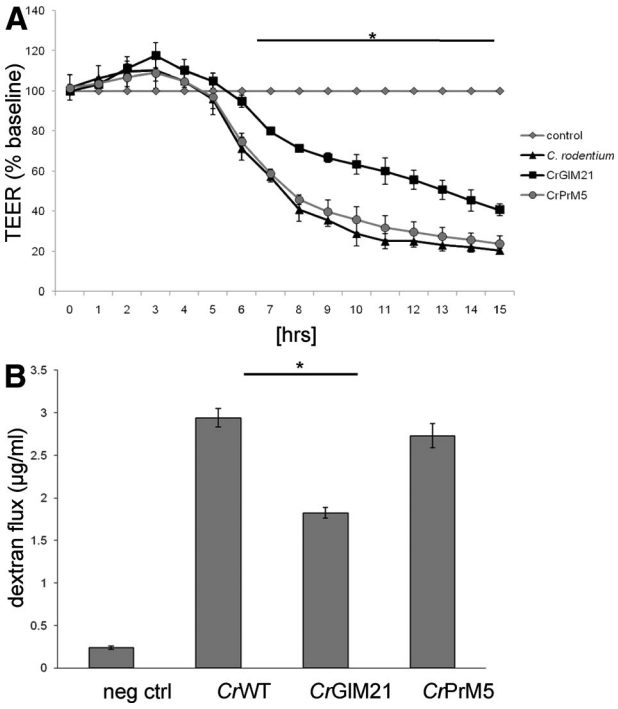

Figure 4. Lymphostatin regulates intestinal epithelial barrier function. **A:** Caco-2 cell monolayers were infected at MOI 10:1 with *C. rodentium* strains for 15 hours. All three strains decreased TEER throughout time, however, infection with *Cr*GIM21 resulted in some attenuation of the decline in TEER, which became significant after 6 hours of infection ($*P < 0.05$). **B:** Caco-2 cell monolayers were infected at MOI 10:1 with *C. rodentium* wild type, *Cr*GIM21, or *Cr*PrM5 for 15 hours. After 5 hours of infection, monolayers were apically loaded with FD-3. Samples were taken from the lower chamber 60 minutes later, and fluorescence intensity determined. Data are expressed as mean with SEM from three individual experiments. In comparison with *C. rodentium* wild type (*Cr*WT) and *Cr*PrM5, dextran flux was reduced in *Cr*GIM21-infected monolayers ($*P < 0.05$).

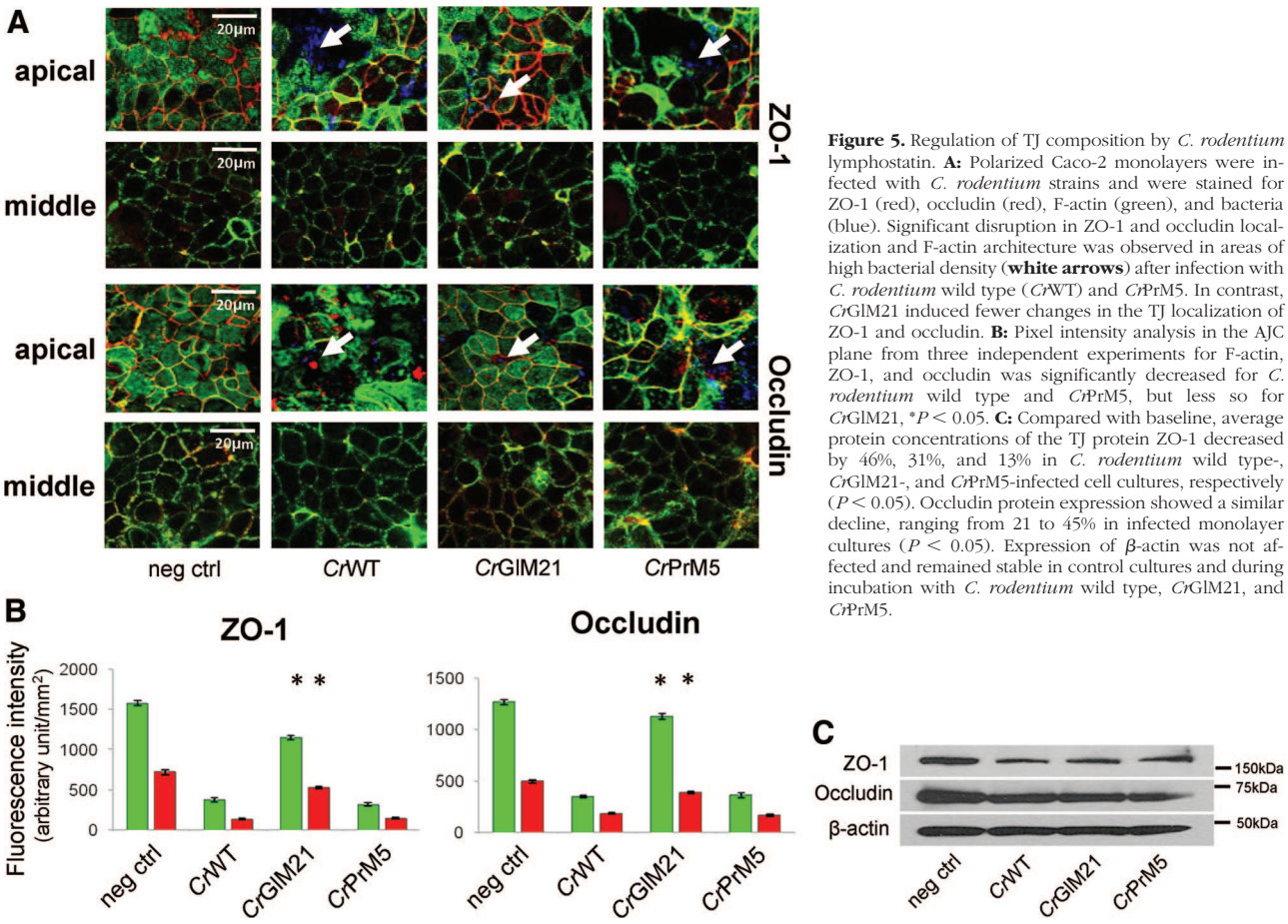

Figure 5. Regulation of TJ composition by *C. rodentium* lymphostatin. **A:** Polarized Caco-2 monolayers were infected with *C. rodentium* strains and were stained for ZO-1 (red), occludin (red), F-actin (green), and bacteria (blue). Significant disruption in ZO-1 and occludin localization and F-actin architecture was observed in areas of high bacterial density (**white arrows**) after infection with *C. rodentium* wild type (*Cr*WT) and *Cr*PrM5. In contrast, *Cr*GlM21 induced fewer changes in the TJ localization of ZO-1 and occludin. **B:** Pixel intensity analysis in the AJC plane from three independent experiments for F-actin, ZO-1, and occludin was significantly decreased for *C. rodentium* wild type and *Cr*PrM5, but less so for *Cr*GlM21, $^*P < 0.05$. **C:** Compared with baseline, average protein concentrations of the TJ protein ZO-1 decreased by 46%, 31%, and 13% in *C. rodentium* wild type-, *Cr*GlM21-, and *Cr*PrM5-infected cell cultures, respectively ($P < 0.05$). Occludin protein expression showed a similar decline, ranging from 21 to 45% in infected monolayer cultures ($P < 0.05$). Expression of β-actin was not affected and remained stable in control cultures and during incubation with *C. rodentium* wild type, *Cr*GlM21, and *Cr*PrM5.

disrupted the localization and expression of TJ and AJ proteins, our findings support that glucosyltransferase motif activity primarily influences TJs, whereas protease motif activity predominantly disrupts the AJ.

Lymphostatin Modulates Rho GTPase Activity

Rho GTPases influence structure and function of the AJC. Furthermore, the glucosyltransferase and protease motif have both been implicated in the regulation of small GTPases, including Rac,[29] RhoA,[30] and Cdc42.[31] We therefore sought to determine whether lymphostatin modulates the activity of Rho GTPases in our system and if lymphostatin-induced changes in their GTPase activity are influencing AJC structure and function after *C. rodentium* infection. Four hours after of infection of polarized Caco-2 monolayers with *C. rodentium* strains, the activation status of Rho and Rac1/Cdc42 were determined. As compared with uninfected epithelial monolayers, incubation with *C. rodentium* wild type resulted in a marked increase in Rho activity and significant suppression of Cdc42 activity (Figure 7A). Based on densitometric analysis, levels of Rho activity were increased 1.5-fold and activated Cdc42 was undetectable compared with control (Figure 7B). Similar to *C. rodentium* wild type, *Cr*GlM21 retained the ability to activate Rho (1.3-fold over normal controls), but lost its suppressive effect on Cdc42 activity. Infection with *Cr*PrM5 resulted in suppression of Cdc42 activity similar to *C. rodentium* wild type, but lost the ability to enhance the activity of Rho. No effects on Rac1 activity was observed after infection with *C. rodentium* wild-type and lymphostatin mutant strains (Figure 7, A and B). Taken together, these data suggest that lymphostatin differentially influences the activity of Rho and Cdc42. More specifically, glucosyltransferase motif activity appears to play a role in the suppression of Cdc42 activity and the protease motif in the activation of Rho during *C. rodentium* infection.

To mechanistically link the changes in AJC structure with the alterations in Rho GTPase activity induced by lymphostatin, rescue experiments were performed by activating Cdc42 signaling or inhibiting Rho activity during *C. rodentium* wild-type infection. Polarized Caco-2 cell monolayers expressing constitutively active Cdc42 (myc-CdcV12) were infected with *C. rodentium* wild type at MOI 1:10. TEER was recorded as percent change from baseline. After a brief increase in TEER, inoculation with *C. rodentium* wild type leads to a steady decline in TEER, which was significant at 8 hours (Figure 8A). Expression of myc-CdcV12 attenuated the decline in TEER induced by *C. rodentium* wild type, which was apparent after 4 hours. To inhibit Rho function during *C. rodentium* infection, polarized Caco-2 cells were pretreated with exotoxin C3 for 2 hours. TEER steadily declined in response to

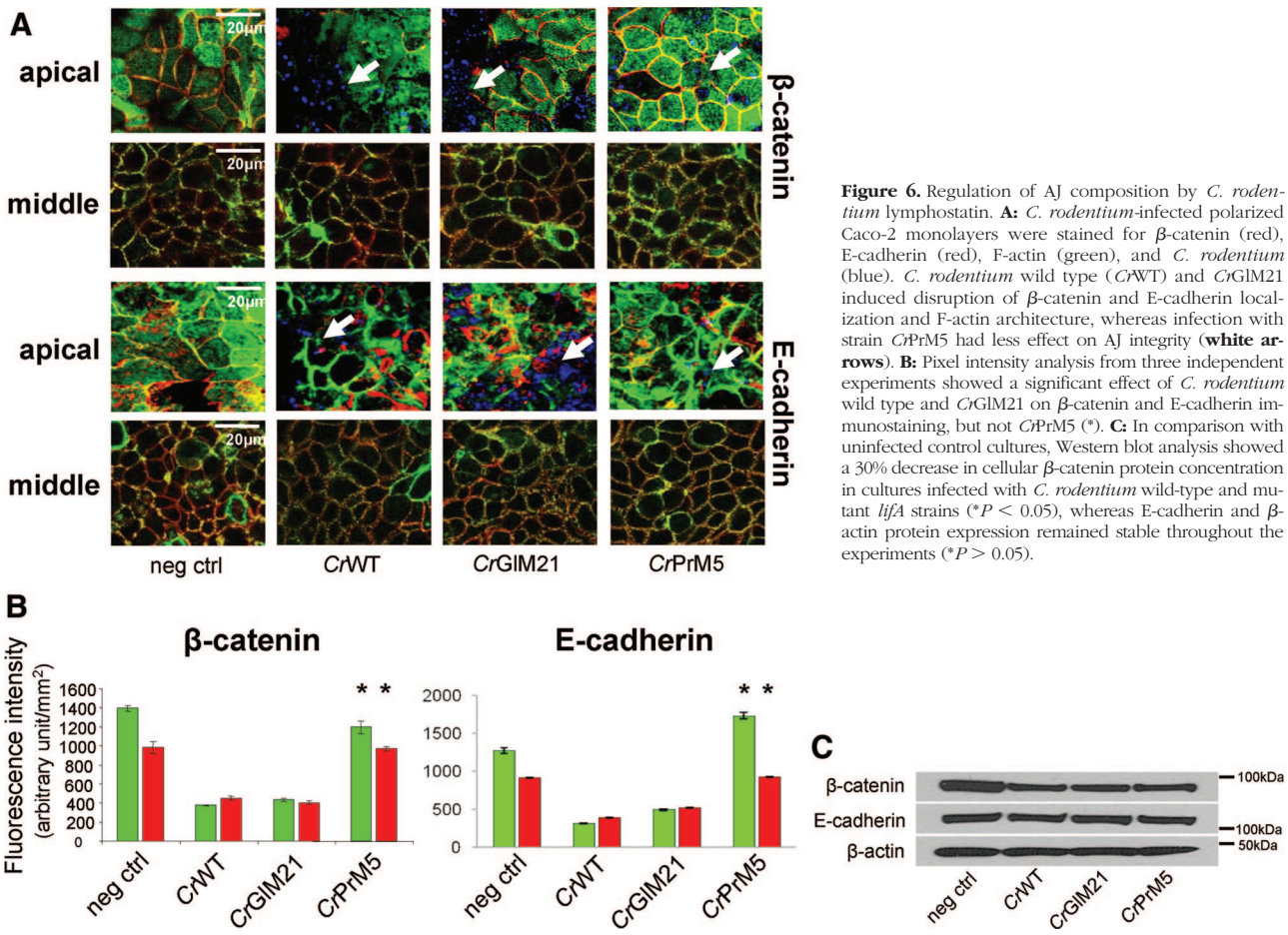

Figure 6. Regulation of AJ composition by *C. rodentium* lymphostatin. **A:** *C. rodentium*-infected polarized Caco-2 monolayers were stained for β-catenin (red), E-cadherin (red), F-actin (green), and *C. rodentium* (blue). *C. rodentium* wild type (*Cr*WT) and *Cr*GIM21 induced disruption of β-catenin and E-cadherin localization and F-actin architecture, whereas infection with strain *Cr*PrM5 had less effect on AJ integrity (**white arrows**). **B:** Pixel intensity analysis from three independent experiments showed a significant effect of *C. rodentium* wild type and *Cr*GIM21 on β-catenin and E-cadherin immunostaining, but not *Cr*PrM5 (*). **C:** In comparison with uninfected control cultures, Western blot analysis showed a 30% decrease in cellular β-catenin protein concentration in cultures infected with *C. rodentium* wild-type and mutant *lifA* strains ($^*P < 0.05$), whereas E-cadherin and β-actin protein expression remained stable throughout the experiments ($^*P > 0.05$).

infection with *C. rodentium* wild type (Figure 8B). However, in the presence of C3 exotoxin, the ability of *C. rodentium* wild type to decrease TEER was abrogated.

We also examined the effect of expression of Cdc42 and C3 exotoxin pretreatment on AJC disruption after infection with *C. rodentium* wild type by confocal microscopy. Both treatments showed an attenuation of the disruption of AJC protein localization and F-actin architecture induced by infection with *C. rodentium* wild type (data not shown). These results suggest that the Rho family of GTPases play a major role in the disruption of epithelial barrier function in response to *C. rodentium* infection. Given our observation with the lymphostatin mutants, we conclude that lymphostatin plays a role in the disruption of intestinal epithelial barrier function *in vitro* via modulation of Rho GTPase activity during infection with *C. rodentium.*

Lymphostatin Plays a Role in the Disruption of the AJC in Vivo

To support our *in vitro* results, we examined the effects of infection with *C. rodentium* wild type and mutants on TJ and AJ structure *in vivo* using our mouse model. Female C57BL/6 mice at 4 weeks of age were infected with 5×10^8 CFU of *C. rodentium* wild type, *Cr*GIM21, and *Cr*PrM5 and infection was allowed proceeding for 8 and 14 days. Distal colonic sections were immunostained for the representative TJ protein occludin and AJ protein β-catenin. Infection with *C. rodentium* wild type and *Cr*PrM5 induced disruption of apically located occludin on day 14, with only minimal changes observed on day 8 after infection (Figure 9, A and B). Infection of mice with *Cr*GIM21 had no identifiable effect on the TJ protein occludin on day 8 or day 14. In contrast, infection with *C. rodentium* wild type and *Cr*GIM21 lead to significant redistribution of β-catenin on day 8 after infection, which recovered by day 14 (Figure 10, A and B). As expected from our *in vitro* experiments, *Cr*PrM5 had no effect on β-catenin on either day 8 or day 14. These *in vivo* results provide validation of our *in vitro* findings and further support that lymphostatin plays a role in the disassembly of the AJC.

Discussion

Previous studies have indicated that infection with *C. rodentium* is not limited to the colon, but also colonizes distant organs.[28] Similarly, we identified *C. rodentium* in mesenteric lymph nodes, spleen, and liver. Interestingly, systemic dissemination of *C. rodentium* was significantly impeded by mutating the *lifA* gene. These findings sug-

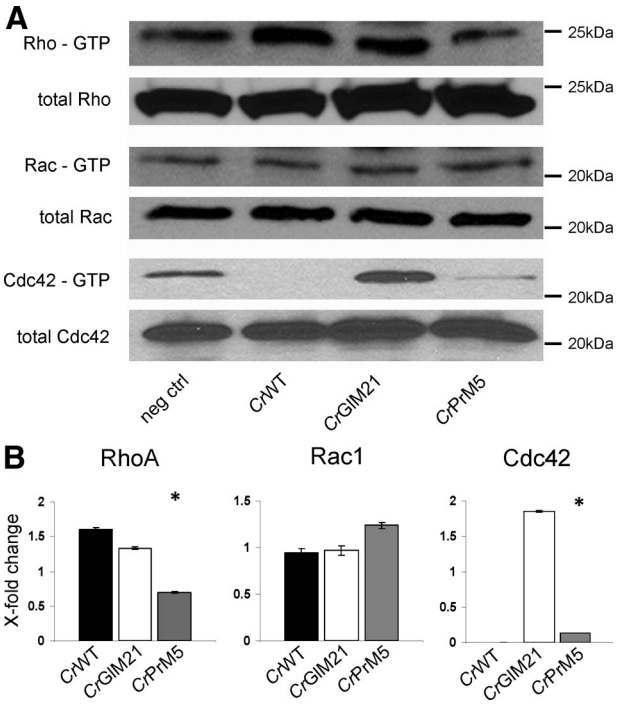

Figure 7. Differential regulation of Rho GTPases by lymphostatin glucosyltransferase and protease motif. In three independent experiments, differentiated Caco-2 monolayer cultures were infected with *C. rodentium* strains at MOI 10:1 for 4 hours. Activated Rho GTPases were isolated and subjected to Western blot analysis (**A**) and pixel analysis (**B**). Infection with *C. rodentium* wild type (*Cr*WT) induced activation of Rho and suppression of Cdc42 activity. Infection with *Cr*PrM5 resulted in reduced Rho activation, whereas infection with *Cr*GlM21 resulted in no suppression of Cdc42 activity (*$P <$ 0.05).

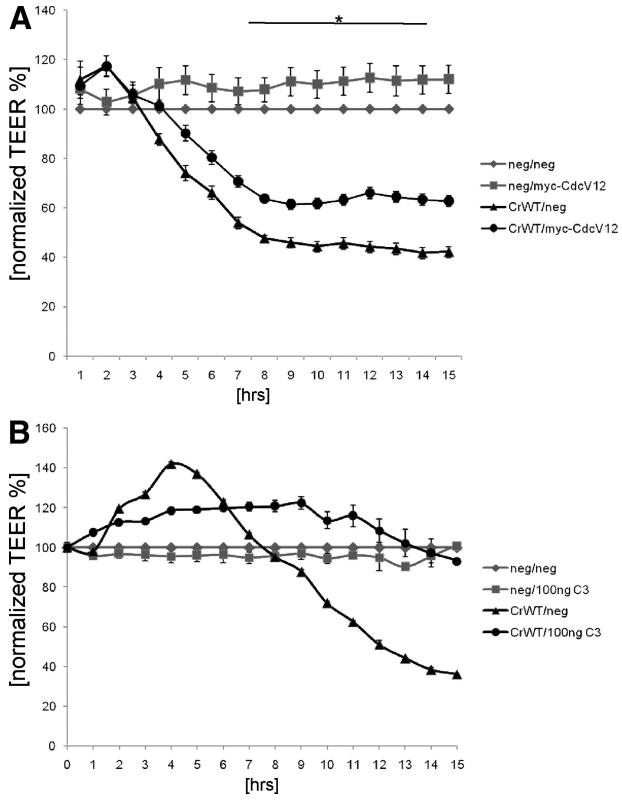

Figure 8. Activation of Cdc42 and inhibition of Rho inhibit loss of TEER after infection with *C. rodentium*. **A:** TEER measurements from three independent experiments with polarized Caco-2 monolayer cultures inoculated with *C. rodentium* wild type (*Cr*WT) (black triangle), expressing myc-CdcV12 (CA-Cdc42, black square) alone, and in combination (black circle). Wild type alone (black triangle) and in combination with myc-CdcV12 (black circle) led to a decrease in TEER throughout time. However, the decrease induced by *C. rodentium* was attenuated in monolayers expressing myc-CdcV12 (black circle). myc-CdcV12 alone (gray square) had a minimal effect on barrier function. **B:** TEER measurements from three independent experiments with polarized Caco-2 monolayer cultures inoculated with *C. rodentium* wild type (black triangle), C3 transferase (gray square) alone, and in combination (black circle). Infection with *C. rodentium* wild type induced a decrease in TEER throughout time. Pretreatment with C3 exotoxin inhibited Rho activity and abrogated the loss of TEER induced by *C. rodentium* wild type (black circle, *$P <$ 0.05).

gested that *C. rodentium* can compromise the intestinal epithelial barrier and implicate lymphostatin in regulating this event. This study focused on determining whether *C. rodentium* can disrupt AJC function and structure and analyzed the role of lymphostatin in this process. Additionally, we investigated the influence of inactivation of lymphostatin glucosyltransferase and protease motifs on bacterial pathogenesis.[21,22]

In addition to influencing cytokine secretion,[7] lymphostatin has also been characterized as an adhesion factor for EHEC serotype O111:H− and was termed *efa-1* (EHEC factor of adherence). Disruption of the *efa-1* gene product resulted in significantly decreased adherence of the bacterium to CHO cells *in vitro*.[25] In contrast to this report, our current results do not suggest significant differences in the number of adherent *C. rodentium* wild-type or lymphostatin mutants to epithelial cells. This is in agreement with our earlier findings reporting that EPEC strain E2348/69 and lymphostatin mutant UMD704 attachment to epithelial cells was indistinguishable.[9] This difference among pathogenic *E. coli* strains might be explained by type IV pilus that is present in *C. rodentium*,[32] E2348/69,[33] and EHEC serotype O157:H7,[34] but not in EHEC serotype O111:H−. It is therefore conceivable that with the exception of EHEC O111:H−, type IV pili function as a primary mechanism for bacterial-epithelial cell adhesion and lymphostatin only fulfills a secondary role for *C. rodentium*, E2348/69, and O157:H7.

Bacterial disruption of intestinal epithelial barrier function is a dynamic process involving multiple bacterial effector proteins and signaling pathways. For example, espF is a type III-dependent protein that induces redistribution of the TJ-associated protein, occludin, with subsequent decrease in TEER.[35] This effect is dependent on a bacterial 14-kDa chaperon protein, rof10, that interacts and increases intracellular espF concentrations.[36] Other molecules that perturb barrier function independent of espF include mitochondria-associated protein[37] and espG in conjunction with orf3.[38] Our findings demonstrate that infection of human intestinal epithelial cells with *C. rodentium* results in disruption of AJC structure and barrier function. These findings are consistent with a recently published report demonstrating that infection of murine intestinal epithelial cells with *C. rodentium* resulted in diminished barrier function associated with disruption of TJ expression of claudins-4 and -5.[39] In addition to disruption of the localization of key AJC proteins, we found that levels of ZO-1, occludin, and β-catenin, but not

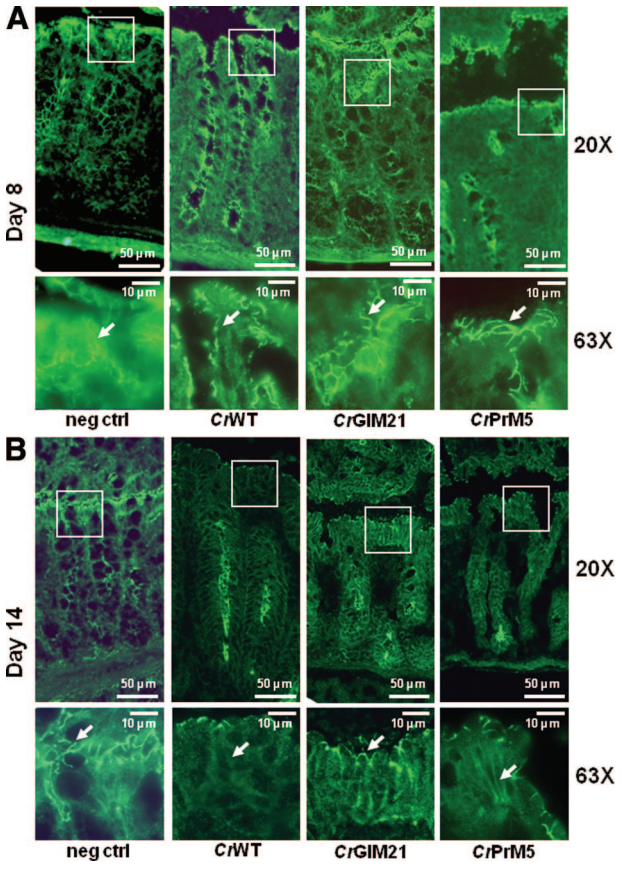

Figure 9. Redistribution of TJ protein occludin *in vivo*. Female C57BL/6 mice were infected with 5×10^8 of either *C. rodentium* wild type (*Cr*WT), *Cr*GlM21, or *Cr*PrM5 by oral gavage. Distal colonic sections were stained for TJ representative protein member occludin and examined on an AxioCam MRc microscope on day 8 (**A**) and day 14 (**B**). In comparison with mice exposed to *C. rodentium* wild type, infection with either *Cr*GlM21 or *Cr*PrM5 led to only minimal changes in occludin distribution on day 8, comparable with negative control (**A**, **white arrows**). However, by day 14, significant disassembly was observed in the colon of *C. rodentium* wild-type and *Cr*PrM5-treated mice, but not during *Cr*GlM21 infection, consistent with *in vitro* experimental findings (**B**, **white arrows**).

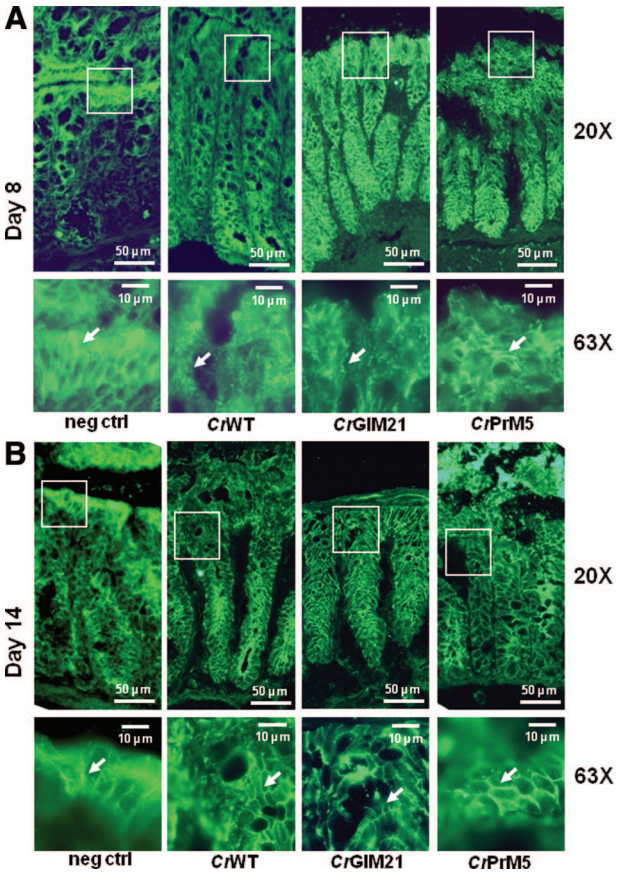

Figure 10. Redistribution of AJ protein β-catenin *in vivo*. Distal colonic sections of C57BL/6 mice infected with 5×10^8 *C. rodentium* wild type (*Cr*WT), *Cr*GlM21, or *Cr*PrM5 were examined for AJ representative protein member β-catenin and examined on an AxioCam MRc microscope on day 8 (**A**) and day 14 (**B**). In comparison with control animals, infection with *C. rodentium* wild type and *Cr*GlM21 induced significant redistribution of β-catenin on day 8 (**A**, **white arrows**), which recovered by day 14 (**B**, **white arrows**) because this AJ protein member was detected predominantly in the membrane fraction. *Cr*PrM5 was unable to displace β-catenin on day 8 or day 14 (**A** and **B**, **white arrows**), confirming earlier *in vitro* results.

E-cadherin or β-actin, were reduced after *C. rodentium* infection. This finding may represent a subsequent degradation of these proteins because of disruption in their localization. However, further studies are required to clarify the mechanisms underlying the reduced expression of these proteins. Additionally, our study suggests that lymphostatin plays a specific role in the disruption of the AJC because mutation of lymphostatin glucosyltransferase and protease motifs differentially influenced how *C. rodentium* influenced distribution of the TJ proteins ZO-1 and occludin, and the AJ proteins β-catenin and E-cadherin. Mutation in the glucosyltransferase motif impaired the ability of *C. rodentium* to influence localization of ZO-1 and occludin at TJs. In contrast, infection with the protease motif mutant strain *Cr*PrM5 resulted in a decrease in the displacement of β-catenin and E-cadherin from the AJ compared with infection with *C. rodentium* wild type. Thus, our findings support that lymphostatin glucosyltransferase activity primarily influences TJs whereas the protease motif activity primarily influences AJs.

A number of signaling pathways known to regulate the AJC, including protein kinase C (PKC) and small GTPases, are targeted by bacterial virulence factors to induce disruption of epithelial barrier function.[40] Previous studies have implicated glucosyltransferase and protease motifs in regulating Rho GTPase family members, including Rac,[29] RhoA,[30] and Cdc42.[31] We observed that infection of Caco-2 monolayers with *C. rodentium* wild type resulted in activation of Rho and suppression of Cdc42 without an effect on Rac1. Mutation of lymphostatin glucosyltransferase motif (*Cr*GlM21) resulted in a loss of the suppression of Cdc42 activity, whereas mutation of the protease motif resulted in loss of increased Rho activation. Together these findings suggest that lymphostatin plays a role in the modulation of Rho GTPase activities. The cycle between the inactive GDP-bound form and active GTP-bound state of these small GTPases are regulated by guanine nucleotide exchange factors and GTPase-activating proteins.[41] Whether lymphostatin interacts directly with Rho and Cdc42 or influences their activity in an indirect manner via interaction with their

regulatory proteins is an important focus for future studies.

Although *C. rodentium* lymphostatin mutants influenced both TJ and AJ components, our data support that the resultant suppression of Cdc42 activity by lymphostatin glucosyltransferase activity primarily disrupts the TJ whereas the activation of Rho by the protease motif primarily disrupts the AJ. However, reports regarding the role of Cdc42 and RhoA in the regulation and maintenance of AJC structure vary. Individual expression of constitutively active or dominant-negative mutants of RhoA, Cdc42, and Rac1 has been shown to disrupt the AJC, albeit with some differences in how they influence AJC protein composition.[42] Recent reports indicated that dominant-active, but not dominant-negative Cdc42, regulates TJ proteins in Madin-Darby canine kidney cells.[43] Consistent with these findings are reports that constitutively active Cdc42 modulates TJ proteins occludin, ZO-1, claudin-1, claudin-2, and junctional adhesion molecule-1.[42] Dominant-negative Cdc42 only had a regulatory effect on claudin-1, but no other members of the TJ. In contrast, overexpression of constitutively active Cdc42 was shown to increase the rate of AJ and TJ formation, whereas inhibition of Cdc42 had the opposite effect.[44] Expression of constitutively active RhoA in MDCK cells resulted in disruption of similar TJ proteins whereas constitutively active Cdc42 had no effect on the composition of the AJ.[42] However, activation of RhoA by cyclooxygenase-2 has been shown to mediate disruption of AJ formation.[45] Such differences in the regulatory roles of these Rho GTPases on TJs and AJs may be related to the characteristics of the particular cell line used and cell density of test cultures. Nonetheless, it appears that a critical balance in the activity of these GTPases determines the integrity of the AJC.

Our rescue experiments with constitutively activated Cdc42 showed attenuation of TEER decrease and changes in the composition of the AJC in response to *C. rodentium* infection. The efficiency of adenoviral infection likely influenced the degree of rescue in these experiments. Rho inactivation with C3 exotoxin completely abrogated the drop in TEER and TJ and AJ protein localization induced by *C. rodentium.* However, our results using lymphostatin mutants suggest that *C. rodentium*-induced Rho activation primarily influences the integrity of the AJ. Because our Rho antibody recognizes RhoA, -B, and -C, these findings may indicate that these GTPases differentially influence AJC composition and function and that *C. rodentium* influences the activity of more than one of these proteins. Further studies are needed to clarify the role of individual Rho proteins in mediating the effects of *C. rodentium* on AJC structure and barrier function. Furthermore, the role of lymphostatin in the regulation of F-actin architecture with subsequent decrease in barrier function needs to be clarified because small GTPases are central in regulating its assembly and disassembly.[46]

Our *in vitro* results were supported by *in vivo* findings in mice infected with *C. rodentium* wild type and mutants showing that the glucosyltransferase activity primarily influences TJs and the protease motif primarily influences AJs. However, in comparison with our *in vitro* results, the timing of the alterations observed in the AJC *in vivo* appeared to be different because β-catenin was redistributed at day 8 whereas occludin was not displaced until day 14 after infection with minimal changes apparent during the time of β-catenin disruption. These differences may be explained by the complexity of multiple cell types in the intestinal mucosa and the complex microenvironment in the mouse colonic mucosa during infection and inflammation.

Given the central role of lymphostatin in the pathogenesis of mouse[10]and human enteric infection with Gram-negative bacteria,[11,47,48] inactivation of either glucosyltransferase or protease motif will result in a significant loss of virulence and susceptibility to host defense mechanisms, including gastrointestinal motility and the mucosal immune system.[49] It is therefore conceivable that therapeutic interventions in the form of specific immunoglobulins directed against lymphostatin and its enzymatic activities might provide an attractive alternative to antibiotics in treating intestinal injury and preventing extraintestinal manifestations of Gram-negative infection.

In summary, our data support that lymphostatin disrupts intestinal epithelial barrier function induced by *C. rodentium* infection via modulating the activity of the small GTPases Rho and Cdc42. Specifically, the glucosyltransferase motif plays a role in the suppression of Cdc42 activity while the protease motif contributes to the activation Rho. These changes in Rho GTPase activity induced by lymphostatin disrupt the AJC and impair intestinal epithelial barrier function.

Acknowledgment

We thank Dr. James Bamburg (Colorado State University, Fort Collins, CO) for the generous gift of the adenoviral vector encoding myc-CdcV12.

References

1. Clarke SC: Diarrhoeagenic Escherichia coli—an emerging problem? Diagn Microbiol Infect Dis 2001, 41:93–98
2. Noël JM, Boedeker EC: Enterohemorrhagic Escherichia coli: a family of emerging pathogens. Dig Dis 1997, 15:67–91
3. Schauer DB, Falkow S: Attaching and effacing locus of a Citrobacter freundii biotype that causes transmissible murine colonic hyperplasia. Infect Immun 1993, 61:2486–2492
4. Deng W, Li Y, Vallance BA, Finlay BB: Locus of enterocyte effacement from Citrobacter rodentium: sequence analysis and evidence for horizontal transfer among attaching and effacing pathogens. Infect Immun 2001, 69:6323–6335
5. Nougayrède JP, Fernandes PJ, Donnenberg MS: Adhesion of enteropathogenic Escherichia coli to host cells. Cell Microbiol 2003, 5:359–372
6. Philpott DJ, McKay DM, Sherman PM, Perdue MH: Infection of T84 cells with enteropathogenic Escherichia coli alters barrier and transport functions. Am J Physiol 1996, 270:G634–G645
7. Klapproth JM, Donnenberg MS, Abraham JM, Mobley HL, James SP: Products of enteropathogenic Escherichia coli inhibit lymphocyte activation and lymphokine production. Infect Immun 1995, 63: 2248–2254
8. Xie G, Bonner CA, Jensen RA: Dynamic diversity of the tryptophan

pathway in chlamydiae: reductive evolution and a novel operon for tryptophan recapture. Genome Biol 2002, 3:research0051
9. Klapproth JM, Scaletsky IC, McNamara BP, Lai LC, Malstrom C, James SP, Donnenberg MS: A large toxin from pathogenic Escherichia coli strains that inhibits lymphocyte activation. Infect Immun 2000, 68:2148–2155
10. Klapproth JM, Sasaki M, Sherman M, Babbin B, Donnenberg MS, Fernandes PJ, Scaletsky IC, Kalman D, Nusrat A, Williams IR: Citrobacter rodentium lifA/efa1 is essential for colonic colonization and crypt cell hyperplasia in vivo. Infect Immun 2005, 73:1441–1451
11. Jores J, Wagner S, Rumer L, Eichberg J, Laturnus C, Kirsch P, Schierack P, Tschape H, Wieler LH: Description of a 111-kb pathogenicity island (PAI) encoding various virulence features in the enterohemorrhagic E. coli (EHEC) strain RW1374 (O103:H2) and detection of a similar PAI in other EHEC strains of serotype 0103:H2. Int J Med Microbiol 2005, 294:417–425
12. Afset JE, Bruant G, Brousseau R, Harel J, Anderssen E, Bevanger L, Bergh K: Identification of virulence genes linked with diarrhea due to atypical enteropathogenic Escherichia coli by DNA microarray analysis and PCR. J Clin Microbiol 2006, 44:3703–3711
13. Anderson JM, Van Itallie CM, Fanning AS: Setting up a selective barrier at the apical junction complex. Curr Opin Cell Biol 2004, 16:140–145
14. Gumbiner BM: Cell adhesion: the molecular basis of tissue architecture and morphogenesis. Cell 1996, 84:345–357
15. Balda MS, Gonzalez-Mariscal L, Matter K, Cereijido M, Anderson JM: Assembly of the tight junction: the role of diacylglycerol. J Cell Biol 1993, 123:293–302
16. Turner JR, Angle JM, Black ED, Joyal JL, Sacks DB, Madara JL: PKC-dependent regulation of transepithelial resistance: roles of MLC and MLC kinase. Am J Physiol 1999, 277:C554–C562
17. Fasano A, Fiorentini C, Donelli G, Uzzau S, Kaper JB, Margaretten K, Ding X, Guandalini S, Comstock L, Goldblum SE: Zonula occludens toxin modulates tight junctions through protein kinase C-dependent actin reorganization, in vitro. J Clin Invest 1995, 96:710–720
18. Kassab Jr F, Marques RP, Lacaz-Vieira F: Modeling tight junction dynamics and oscillations. J Gen Physiol 2002, 120:237–247
19. Saha C, Nigam SK, Denker BM: Involvement of Galphai2 in the maintenance and biogenesis of epithelial cell tight junctions. J Biol Chem 1998, 273:21629–21633
20. Hopkins AM, Li D, Mrsny RJ, Walsh SV, Nusrat A: Modulation of tight junction function by G protein-coupled events. Adv Drug Deliv Rev 2000, 41:329–340
21. Just I, Gerhard R: Large clostridial cytotoxins. Rev Physiol Biochem Pharmacol 2004, 152:23–47
22. Shao F, Merritt PM, Bao Z, Innes RW, Dixon JE: A Yersinia effector and a Pseudomonas avirulence protein define a family of cysteine proteases functioning in bacterial pathogenesis. Cell 2002, 109:575–588
23. Datsenko KA, Wanner BL: One-step inactivation of chromosomal genes in Escherichia coli K-12 using PCR products. Proc Natl Acad Sci USA 2000, 97:6640–6645
24. Zobiack N, Rescher U, Laarmann S, Michgehl S, Schmidt MA, Gerke V: Cell-surface attachment of pedestal-forming enteropathogenic E. coli induces a clustering of raft components and a recruitment of annexin 2. J Cell Sci 2002, 115:91–98
25. Nicholls L, Grant TH, Robins-Browne RM: Identification of a novel genetic locus that is required for in vitro adhesion of a clinical isolate of enterohaemorrhagic Escherichia coli to epithelial cells. Mol Microbiol 2000, 35:275–288
26. Sanders SE, Madara JL, McGuirk DK, Gelman DS, Colgan SP: Assessment of inflammatory events in epithelial permeability: a rapid screening method using fluorescein dextrans. Epithelial Cell Biol 1995, 4:25–34
27. Kuhn TB, Brown MD, Wilcox CL, Raper JA, Bamburg JR: Myelin and collapsin-1 induce motor neuron growth cone collapse through different pathways: inhibition of collapse by opposing mutants of rac1. J Neurosci 1999, 19:1965–1975
28. Brennan PC, Fritz TE, Flynn RJ, Poole CM: Citrobacter freundii associated with diarrhea in a laboratory mice. Lab Anim Care 1965, 15:266–275
29. Just I, Selzer J, Hofmann F, Green GA, Aktories K: Inactivation of Ras by Clostridium sordellii lethal toxin-catalyzed glucosylation. J Biol Chem 1996, 271:10149–10153
30. Just I, Selzer J, Wilm M, von Eichel-Streiber C, Mann M, Aktories K: Glucosylation of Rho proteins by Clostridium difficile toxin B. Nature 1995, 375:500–503
31. Shao F, Vacratsis PO, Bao Z, Bowers KE, Fierke CA, Dixon JE: Biochemical characterization of the Yersinia YopT protease: cleavage site and recognition elements in Rho GTPases. Proc Natl Acad Sci USA 2003, 100:904–909
32. Mundy R, Pickard D, Wilson RK, Simmons CP, Dougan G, Frankel G: Identification of a novel type IV pilus gene cluster required for gastrointestinal colonization of Citrobacter rodentium. Mol Microbiol 2003, 48:795–809
33. Stone KD, Zhang HZ, Carlson LK, Donnenberg MS: A cluster of fourteen genes from enteropathogenic Escherichia coli is sufficient for the biogenesis of a type IV pilus. Mol Microbiol 1996, 20:325–337
34. Xicohtencatl-Cortes J, Monteiro-Neto V, Ledesma MA, Jordan DM, Francetic O, Kaper JB, Puente JL, Giron JA: Intestinal adherence associated with type IV pili of enterohemorrhagic Escherichia coli O157:H7. J Clin Invest 2007, 117:3519–3529
35. McNamara BP, Koutsouris A, O'Connell CB, Nougayrede JP, Donnenberg MS, Hecht G: Translocated EspF protein from enteropathogenic Escherichia coli disrupts host intestinal barrier function. J Clin Invest 2001, 107:621–629
36. Elliott SJ, O'Connell CB, Koutsouris A, Brinkley C, Donnenberg MS, Hecht G, Kaper JB: A gene from the locus of enterocyte effacement that is required for enteropathogenic Escherichia coli to increase tight-junction permeability encodes a chaperone for EspF. Infect Immun 2002, 70:2271–2277
37. Dean P, Kenny B: Intestinal barrier dysfunction by enteropathogenic Escherichia coli is mediated by two effector molecules and a bacterial surface protein. Mol Microbiol 2004, 54:665–675
38. Tomson FL, Viswanathan VK, Kanack KJ, Kanteti RP, Straub KV, Menet M, Kaper JB, Hecht G: Enteropathogenic Escherichia coli EspG disrupts microtubules and in conjunction with Orf3 enhances perturbation of the tight junction barrier. Mol Microbiol 2005, 56:447–464
39. Flynn AN, Buret AG: Tight junctional disruption and apoptosis in an in vitro model of Citrobacter rodentium infection. Microb Pathog 2008, 45:98–104
40. Matsuzawa T, Kuwae A, Abe A: Enteropathogenic Escherichia coli type III effectors EspG and EspG2 alter epithelial paracellular permeability. Infect Immun 2005, 73:6283–6289
41. Mackay DJ, Hall A: Rho GTPases. J Biol Chem 1998, 273: 20685–20688
42. Bruewer M, Hopkins AM, Hobert ME, Nusrat A, Madara JL: RhoA, Rac1, and Cdc42 exert distinct effects on epithelial barrier via selective structural and biochemical modulation of junctional proteins and F-actin. Am J Physiol 2004, 287:C327–C335
43. Rojas R, Ruiz WG, Leung SM, Jou TS, Apodaca G: Cdc42-dependent modulation of tight junctions and membrane protein traffic in polarized Madin-Darby canine kidney cells. Mol Biol Cell 2001, 12:2257–2274
44. Fukuhara A, Shimizu K, Kawakatsu T, Fukuhara T, Takai Y: Involvement of nectin-activated Cdc42 small G protein in organization of adherens and tight junctions in Madin-Darby canine kidney cells. J Biol Chem 2003, 278:51885–51893
45. Chang YW, Marlin JW, Chance TW, Jakobi R: RhoA mediates cyclooxygenase-2 signaling to disrupt the formation of adherens junctions and increase cell motility. Cancer Res 2006, 66:11700–11708
46. Vandenbroucke E, Mehta D, Minshall R, Malik AB: Regulation of endothelial junctional permeability. Ann NY Acad Sci 2008, 1123:134–145
47. Karmali MA, Mascarenhas M, Shen S, Ziebell K, Johnson S, Reid-Smith R, Isaac-Renton J, Clark C, Rahn K, Kaper JB: Association of genomic O island 122 of Escherichia coli EDL 933 with verocytotoxin-producing Escherichia coli seropathotypes that are linked to epidemic and/or serious disease. J Clin Microbiol 2003, 41:4930–4940
48. Wickham ME, Lupp C, Mascarenhas M, Vazquez A, Coombes BK, Brown NF, Coburn BA, Deng W, Puente JL, Karmali MA, Finlay BB: Bacterial genetic determinants of non-O157 STEC outbreaks and hemolytic-uremic syndrome after infection. J Infect Dis 2006, 194:819–827
49. MacDonald TT: The mucosal immune system. Parasite Immunol 2003, 25:235–246